Environmental Science & Policy 59 (2016) 1–9

Contents lists available at ScienceDirect

Environmental Science & Policy

journal homepage: www.elsevier.com/locate/envsci

Flood inundation uncertainty: The case of a 0.5% annual probability flood event

Thomas Prime[a,b,*], Jennifer M. Brown[b], Andrew J. Plater[a]

[a] School of Environmental Sciences, University of Liverpool, UK
[b] National Oceanography Centre, Liverpool, UK

ARTICLE INFO

Article history:
Received 24 September 2015
Received in revised form 20 January 2016
Accepted 25 January 2016
Available online 3 February 2016

Keywords:
Flood hazard
Uncertainty
Coastal defences
Resilience
Cost-effective
Joint probability

ABSTRACT

Aging coastal defences around the UK are challenging managers to redesign schemes to be resilient to extreme events and climate change, be cost-effective, and have minimal or beneficial environmental impact. To enable effective design, reduced uncertainty in the assessment of flood risk due to natural variability within the coastal forcing is required to focus on conditions that pose highest threat. The typical UK standard of protection for coastal defences is to withstand a 0.5% annual probability event, historically also known as a 1 in 200 year return period event. However, joint wave-water level probability curves provide a range of conditions that meet this criterion. We examine the Dungeness and Romney Marsh coastal zone, a region of high value in terms of habitat and energy assets, to quantify the uncertainty in flood depth and extent generated by a 0.5% probability event, and to explore which combinations of wave and water levels generate the greatest threat.

1. Introduction

Coastal managers must consider many different aspects when planning new coastal defence schemes to maintain resilience to coastal flooding in locations with aging defence structures. New structures need to be resilient to extreme events and the impacts of climate change over the defences' design life, typically 75–100 years (Buijs et al., 2007). However, new schemes also need to be cost-effective and implemented in a timely manner to reduce the economic impact of future extreme events. This means an understanding of the probability of both the extreme events occurring and a defence being exceeded is required (Buijs et al., 2007). To enable effective adaptation, better understanding of the uncertainty associated with the flood hazard of an event due to variability in conditions is required to enable implementation of cost-effective design (Wadey et al., 2013).

Sources of coastal flooding are varied and range from contributions to the water level, such as astronomical tides and storm surges (McMillan et al., 2011), to wave run-up and overwashing or overtopping, driven by the coincidental wave conditions. A storm surge occurs when high winds and low atmospheric pressure act on the sea surface to cause a temporary increase in water level (Wells, 2011). If this occurs in conjunction with a high tide, particularly a spring tide, an extreme still water level (EWL) event arises. EWLs will have an increased impact (McInnes et al., 2003) and increased probability of occurrence (Prime et al., 2015) in the future due to rising mean sea level. Wind waves, generated locally, or swell waves, generated by an offshore storm, impacting a coastline at the same time as the EWL, will increase the observed water level at the shoreline above the EWL alone due to wave run-up and set-up (Longuet-Higgins, 1970), further increasing the impact of the extreme event (Chini and Stansby, 2012).

This paper demonstrates the uncertainty in flood hazard due to variability within the combined forcing of extreme events. The UK design standard for sea defences varies depending on asset being protected, for example, nuclear power stations are designed to be resilient to a 1 in 10,000 year event but a typical design tolerance for urban areas is a 1 in 200 year event, or a 0.5% annual probability of occurrence (Wyse, 2015). This design standard can be applied using one variable such as EWL, which has been calculated at a national scale for 16 return periods of extreme water levels (McMillan et al., 2011). A more comprehensive standard is one that considers both water level (WL) and significant wave height (*Hs*) occurring together. This can then be used to understand further contributions to coastal flooding such as wave run-up. Combining two variables in this way is known as multivariate probability analysis or joint probability analysis (Coles and Tawn, 1990). In the context of WL and *Hs*, joint probability methods were rare until the 1980's rare due to the lack of long-term wave data and suitable

* Corresponding author.
E-mail address: tprime@liv.ac.uk (T. Prime).

http://dx.doi.org/10.1016/j.envsci.2016.01.018

statistical tools. Therefore, the standard process was to consider the wave and water levels separately (Hames and Reeve, 2007). As it became clear that there was a need for better understanding of joint probability, research was undertaken to overcome these barriers (Hawkes and Svensson, 2006) resulting in the development of specialist joint probability analysis software, JOIN-SEA; used by industry as well as academic researchers and also for the research in this paper (Hawkes and Gouldby, 1998).

Using the joint probability of WL and *Hs* is more representative of an extreme event than combining the *Hs* and EWL of a given return period calculated in isolation. Classifying the joint conditions as well as their probability of occurrence provides a better understanding of how resilient current defences are to extreme events (Wadey et al., 2015). However, different combinations of *Hs* and WL can have the same joint probability of occurrence. The varying impacts from these different combinations of a given return period have not been examined before.

For this study we selected the annual probability of 0.5%, or 1 in 200 years in return period (RP) terminology, representative of a typical UK standard of defence. This is consistent with the UK Environment Agency flood mapping service that shows areas benefiting from flood defences at this annual probability of

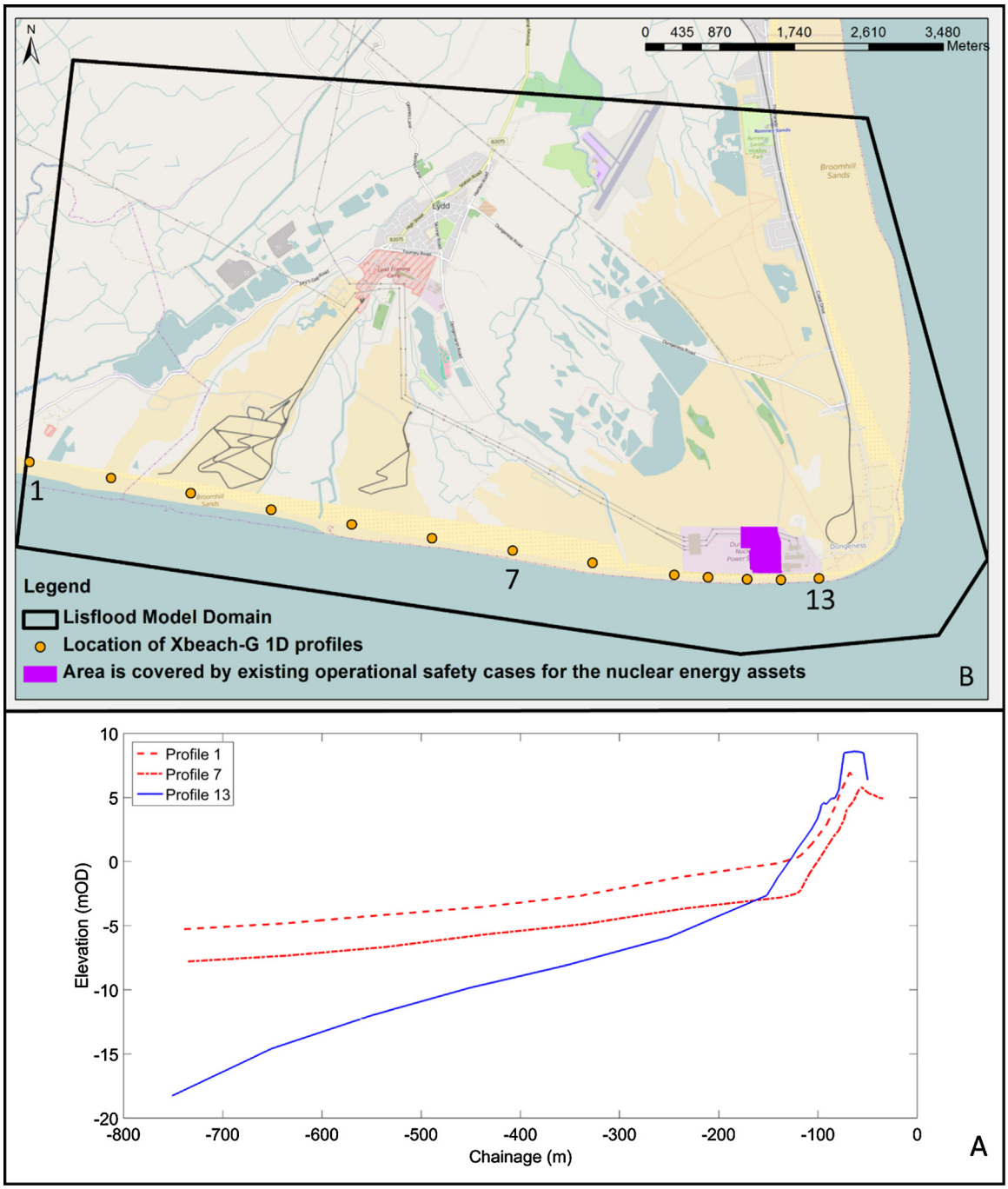

Fig. 1. (A) Beach profiles showing the shoreline variability, the red lines (profile 1 and 7) represent the natural defences and the blue line (profile 13) represents the engineered defences fronting the power stations.**1B**: Dungeness and Romney Marsh; the black line shows the model boundary. The orange dots denote the beach profiles used within the storm impact model. The area shaded in purple is covered by existing operational safety cases for the nuclear energy assets. (For interpretation of the references to colour in this figure legend, the reader is referred to the web version of this article.)

occurrence (Wyse, 2015). The objective of this study is to show that there is uncertainty in the inundation extent and flood depths for conditions that are all similarly classified as a 0.5% probability event at a given location. This will inform coastal managers of the most hazardous combinations of events that attain this probability of occurrence for the purpose of designing new build or maintenance schemes to withstand a specific standard of protection.

2. Study site

The study site selected, Dungeness and Romney Marsh (Fig. 1B), is a region of the UK that has a high value both in terms of protected habitat and important energy infrastructure. It is also an internationally important location for geomorphology, plant and invertebrate communities as well as birdlife (JNCC, 2015; Long et al., 2007). It is part of a designated Site of Scientific Special Interest (SSSI), which covers Dungeness, Romney Marsh and Rye Bay (Natural England, 2015). The maximum predicted tidal range at Dungeness is 8.6 m, with a mean high water spring tide of 3.54 m OD (Ordnance Datum), with a highest predicted tide of 4.48 m OD (NTSLF, 2015). The closest tide gauge at Dover shows that storm surges can reach up to 1.6 m (BODC, 2015). The closest wave buoy shows that the most common wave directions are from the southwest and the northeast, with the southwest being associated with the largest waves up to 5 m high and peak periods (*Tp*) of up to 18 seconds (Mason et al., 2009). The typical direction for coastal wave impact on the southern shoreline is from the southwest, due to the orientation of the peninsula.

Dungeness has both 'natural' defences in the form of a maintained gravel barrier, and engineered structures (e.g., Fig. 1A). Better understanding of the uncertainty of the flood hazard to the region is critical in managing human intervention within the nature reserve and in maintaining resilience for the nearby operational power station which is currently licenced to operate beyond 2018 (EDF, 2012). As it is a licensed nuclear site there will be a nuclear installation here undergoing decommissioning up to and beyond 2100.

The defences along Dungeness southern shore comprise gravel beaches with a secondary defence behind that consists of an earth embankment known locally as the 'Green Wall'. At the western end the Green Wall is immediately behind the beach and at the eastern end it is setback several hundred metres. In front of the energy infrastructure there is a large gravel barrier that has been augmented to provide a standard of protection to a 1 in 10,000 year event. The current defence policy for these defences is 'Hold the Line'.

3. Methodology

This study investigates 30 different combinations of *Hs* and WL with the same annual probability of occurrence, allowing the assessment of uncertainty in the 0.5% extreme event under present-day sea level. The approach combines a storm impact model with a flood inundation model. The storm impact model is able to take wave climate parameters and, when combined with a time-varying WL, output the overwashing discharge at the defence crest of a 1D beach profile. This feeds into the flood inundation model as a boundary condition, for the duration overwashing occurs, thus simulating the inundation extent and volume for that *Hs* and WL combination.

The outputs from the inundation model show the uncertainty around a 0.5% event and how the inundation and overwashing rates can vary depending on the input *Hs* and EWL combinations. The domain considered in the flood inundation model (Fig. 1B) covers both nuclear sites on Dungeness foreland at the eastern end

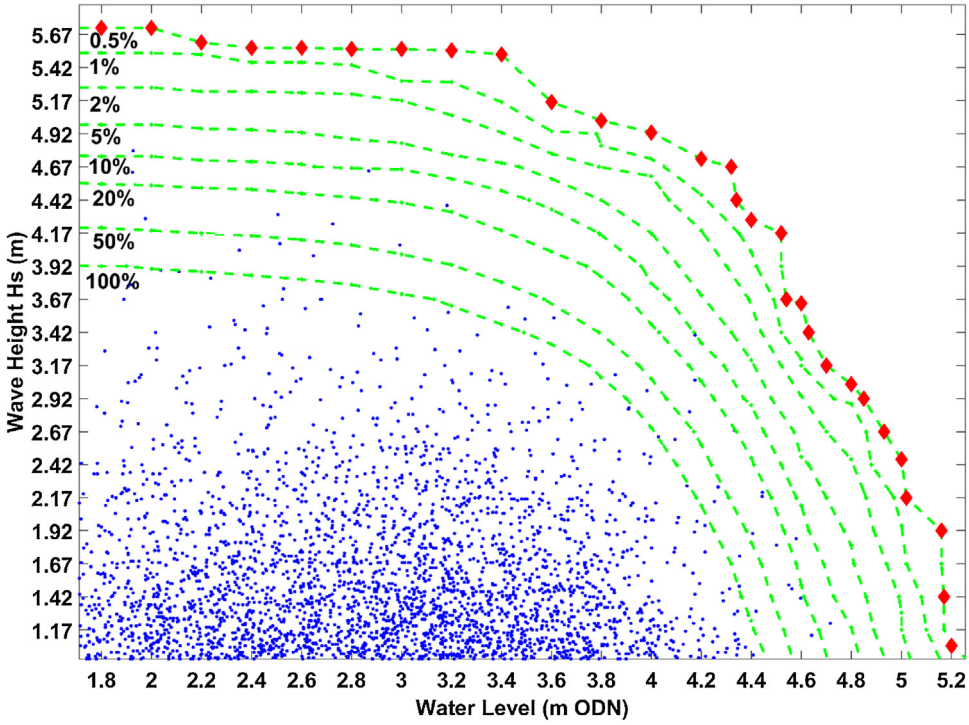

Fig. 2. Joint Hs and WL probability curves (green lines) of the observed conditions at Dungeness (blue dots). The annual probability of occurrence shown range from 100% up to 0.5%. The blue dots are wave height and water observations. Red diamonds show the 30 selected combinations of wave height and EWL that will be modelled. (For interpretation of the references to colour in this figure legend and the text, the reader is referred to the web version of this article.)

of this section of the coastline (Dungeness Point), and runs west through Denge Marsh, past Holmstone to Jury's Gap. The town of Lydd is also within the flood domain.

3.1. Joint probability of extreme wave height and water level

To calculate joint probability a dataset of *Hs* and *Tp* at high water along with the corresponding WL is needed. The UK has a WaveNet system of nearshore buoys that have been deployed since 2002 and are maintained by the Centre for Environment, Fisheries and Aquaculture Science (Cefas). The closest buoy to the study site is located at Hastings, which has collected data from 26th November 2002 (Cefas, 2015). The tide gauge at Dover was used to provide the observed water elevation data. It is part of the UK tide gauge network, comprising 43 gauges that are maintained and quality controlled by the British Oceanographic Data Centre (BODC).

The *Hs* during each observed high water was used in a joint probability program, JOIN-SEA (Hawkes and Gouldby, 1998), which has been extensively used and is well validated (Hawkes and Svensson, 2006). The approach JOIN-SEA uses is based on proposals by (Coles and Tawn, 1990). This is where a bivariate or a mixture of two bivariate probability distributions is fitted to the largest values or upper tail of the wave height and water level dataset. The outputs from JOIN-SEA are presented as joint probability curves (Fig. 2).

The return period curve (Fig. 2) shows the range of *Hs* and WL that could potentially occur with a probability of 0.5%. With increasing WL, a lower *Hs* is required to achieve the 0.5% probability level. Table 1 lists the combinations (shown in Fig. 2 as red diamonds) that are modelled to show the uncertainty in flood inundation for this return level.

The *Tp* were selected using observed wave conditions. The data have two clear linear relations (not shown) between the *Hs* and *Tp*, representing locally generated and swell wave conditions. Longer period waves are associated with larger wave run-ups and wave overwashing of defences (Palmer et al., 2014). Therefore, to maximise impact, the longest *Tp* wave for each *Hs* was selected, creating wave events which were considered to represent the greatest flood hazard. Due to the need to maximise the number of data inputs within the limited data record the full dataset was used. As the highest waves originate from the southwest, which directly impact the coastline studied, the joint probability curves are unlikely to be overestimated.

3.2. Synthetic storm tide

The WL, described in Section 3.1, is converted into a time-varying water elevation that comprises of a combination of storm surge and tide that peaks at the required WL. The dataset provided by (McMillan et al., 2011) provides synthetic scaled storm surge curves for each tide gauge location around the UK. Using the WLs combined with the synthetic storm surge curve for Dover 30 km away, as suggested for the region by (McMillan et al., 2011), and a locally predicted spring tide, a time-varying WL that peaks at the desired level for each scenario was produced. This was used as an input parameter for the storm impact model. Although uncertainty in flood hazard can also be linked to the choice of surge curve (Quinn et al., 2014), a single curve with the peak of the surge assumed to occur at the same time as tidal high water was adopted following the methodology of (McMillan et al., 2011). This approach is likely to overestimate the hazard of the WL as it is unlikely that the peak surge will occur at tidal high water. Given that this study is focussed on the uncertainty in the combination of events the approach of aligning the tide and surge peaks is considered to be appropriate.

Table 1
List of wave height and water elevations with the incremental change in each parameter representing the 30 selected 0.5% event probability events.

Scenario number	Significant wave height (m)	Change in wave height (m)	Peak wave period (s)	Change in period (s)	Water elevation (m)	Change in water elevation (m)
1	5.72	N/A	10	N/A	1.8	N/A
2	5.72	0	10	0	2	0.2
3	5.61	−0.11	10	0	2.2	0.2
4	5.57	−0.04	10	0	2.4	0.2
5	5.57	0	10	0	2.6	0.2
6	5.56	−0.01	10	0	2.8	0.2
7	5.56	0	10	0	3	0.2
8	5.55	−0.01	10	0	3.2	0.2
9	5.52	−0.03	9.1	−0.9	3.4	0.2
10	5.16	−0.36	8.3	−0.8	3.6	0.2
11	5.02	−0.14	10	1.7	3.8	0.2
12	4.93	−0.09	10	0	4	0.2
13	4.73	−0.2	9.1	−0.9	4.2	0.2
14	4.67	−0.06	10	0.9	4.32	0.12
15	4.42	−0.25	10	0	4.34	0.02
16	4.27	−0.15	10.5	0.5	4.4	0.06
17	4.17	−0.1	9.1	−1.4	4.52	0.12
18	3.67	−0.5	10	0.9	4.54	0.02
19	3.64	−0.03	10	0	4.6	0.06
20	3.42	−0.22	10.5	0.5	4.63	0.03
21	3.17	−0.25	10.5	0	4.7	0.07
22	3.03	−0.14	10	−0.5	4.8	0.1
23	2.92	−0.11	10	0	4.85	0.05
24	2.67	−0.25	10.5	0.5	4.93	0.08
25	2.46	−0.21	10.5	0	5	0.07
26	2.17	−0.29	10	−0.5	5.02	0.02
27	1.92	−0.25	10	0	5.16	0.14
28	1.42	−0.5	10	0	5.17	0.01
29	1.05	−0.37	13.3	3.3	5.2	0.03
30	0.92	−0.13	16.7	3.4	5.28	0.08

3.3. Storm impact model

XBeach-G is the storm impact model used to simulate the overwashing of defences in the study area (Fig. 1). XBeach-G simulates storm impacts on gravel barrier beaches (McCall et al., 2014). It currently consists of a 1D model that is able to simulate the discharge over a defence crest. As the defences at Dungeness are primarily composed of a gravel barrier, this makes XBeach-G highly suitable for this work (McCall et al., 2015, 2014).

To represent alongshore coastal variability, 13 transects along the modelled coastline (Fig. 1B) are located at approximately 1 km intervals. The inputs used to force the model are the synthetic storm tide curve (see Section 3.2) and the *Hs* and *Tp* (see Section 3.1). The storm impact model derives a JONSWAP wave spectrum based on the wave values. Wave direction was not taken into account during the XBeach-G simulations. The final input is the beach profile, (Fig. 1A). At Dungeness regular beach profiles at 50 m intervals are available. Selected beach profiles were extended with offshore bathymetry to determine the sub-tidal profile gradient. For Dungeness this profile becomes steeper and deeper the further east along the coastline. The bathymetry extends 1 km offshore which allows the use of offshore waves and surge curves. Each of the 13 profiles were used in Xbeach-G simulations of each of the 30 0.5% probability scenarios, to produce the overwash discharge at a defined point for the current defences.

XBeach-G calculates the evolution of the beach profile over the course of the simulation; a value of 0.025 m was used for the D_{50} (Dombusch et al., 2003). Morphological change was enabled for the simulations in this study as it is important to allow the defence profile to change during the simulation as additional protection from an increase in the crest height due to wave action would be beneficial. The discharge in $m^2 s^{-1}$ per metre of the defence simulated by XBeach-G for the 13 profiles provided a spatially variable overwashing discharge of the defences suitable to use as a boundary condition at the crest level of the defences in the inundation model.

3.4. Flood inundation model

The flood inundation model used was LISFLOOD-FP; this is a two dimensional finite difference hydrodynamic model based on the storage cell approach. LISFLOOD-FP has been successful in coastal applications, and offers a good fit between observed and predicted inundation extents (Skinner et al., 2015). This model was first formulated by (Bates and De Roo, 2000) and is capable of being computationally efficient while running on high resolution LiDAR model domains (Bates et al., 2010). The LiDAR data for the domain covering the Dungeness and Romney Marsh area were provided at a horizontal resolution of 2 m by the Environment Agency Geomatics department. The key requirements for LISFLOOD-FP to ensure a good model simulation is an accurate terrain model (provided by the EA LiDAR), boundary forcing (provided by XBeach-G, as described in Section 3.3) and a friction parameter that determines how quickly water will flow from model cell to cell. The domain under study has limited urbanisation and there are no forests or salt marshes requiring high friction areas, hence a single value typical of the main gravel terrain was used. Sensitivity analysis was performed with an example inundation scenario (Number 14, Table 1) being run with high (0.1 Manning's *n* typical value for a forest) and a low (0.018 Manning's *n* typical urban value) values of friction. Outputs from this analysis were compared with that produced using a 0.04 value of Manning's *n*, which represents gravel areas. The percentage difference in extent between each of the three different friction value simulations was of the order of ±0.04%. Therefore, the domain is considered to be insensitive to the friction parameter and 0.04 was suitable to use as the single parameter for friction. The LiDAR was resampled to 5 m horizontal resolution to improve computational efficiency while maintaining a high resolution to accurately capture the inundation extent and capture the defence crests within the model domain.

The model outputs the flood water depths at the maximum simulated inundation extent at 5 m horizontal resolution, and the maximum hazard map during the duration of the simulation.

The hazard in relation to danger to people is calculated for each grid cell at each time-step using the rating in Table 2 following equation based on (Ramsbottom, 2003):

$$Hazard = (WaterDepth \times (Water\,Velocity + 1.5)) \quad (1)$$

This constant in Eq. (1) has been added to compensate for the fact that flood water depths with low or zero velocities are still hazardous, but very low flood water depths are not regardless of the water velocity.

4. Results

4.1. Modelled inundation values

The results for all 30 scenarios include the: 5th, 50th and 95th percentile values of water depth and hazard (Fig. 3A and B), inundation area and volume (Fig. 3 C) and mean discharge over the simulation across all 13 profiles (Fig. 3D).

The general trend across Fig. 3A and C is increasing hazard value, water depth, area, volume and mean discharge with increasing scenario number, which corresponds to increasing WL and decreasing *Hs*. Fig. 3D shows a generally increasing trend of mean overwash discharge to scenario 15. To this point increasing WL has more influence on the overwash discharge than the decreasing *Hs*, and vice versa after this point as the discharge decreases. Scenario 29 and 30 suddenly show high rates of discharge again as the wave regime becomes swell dominant (with long periods). Fig. 4 shows an example of the flood extent outlines from the 30 scenarios (Table 1). The minimum and maximum extent (3 and 30), and two tipping points in the inundation extent, a large increase (10 and11) and a large decrease (16 and 17), are shown. The general trend is of increasing extent but there is variability.

4.2. Variation in inundation area and volume

Fig. 4 shows a significant variation in inundation extent between the maximum (red outline) and minimum extent (black outline). It also shows spatial variation in the number of overwash locations along the coastline in relation to variability in the beach/defence profile. The overwashing discharge rates also vary for different *Hs* and WL combinations that have the same annual joint probability of occurrence. Areas with lower crest level or that evolve to have a lower crest level enable overwash fans (Bradbury and Powell, 1992). Fan occurrences become more widespread and increase in size with increasing extreme water level. As morphology has been enabled for the simulations in XBeach-G, this allows the potential for the crest level to lower. Ideally repeat simulations would have been undertaken with the morphology turned off to

Table 2
Hazard value categories and their meaning for the general public, emergency services and vulnerable people (elderly and children) (Ramsbottom, 2003).

Hazard value	Category
Hazard value >2.0	Danger for all (including emergency services
1.25< Hazard value ≤2.0	Danger for most (general public)
0.75< Hazard value ≤1.25	Danger for some (elderly and children)
Hazard value ≤0.75	Very low danger

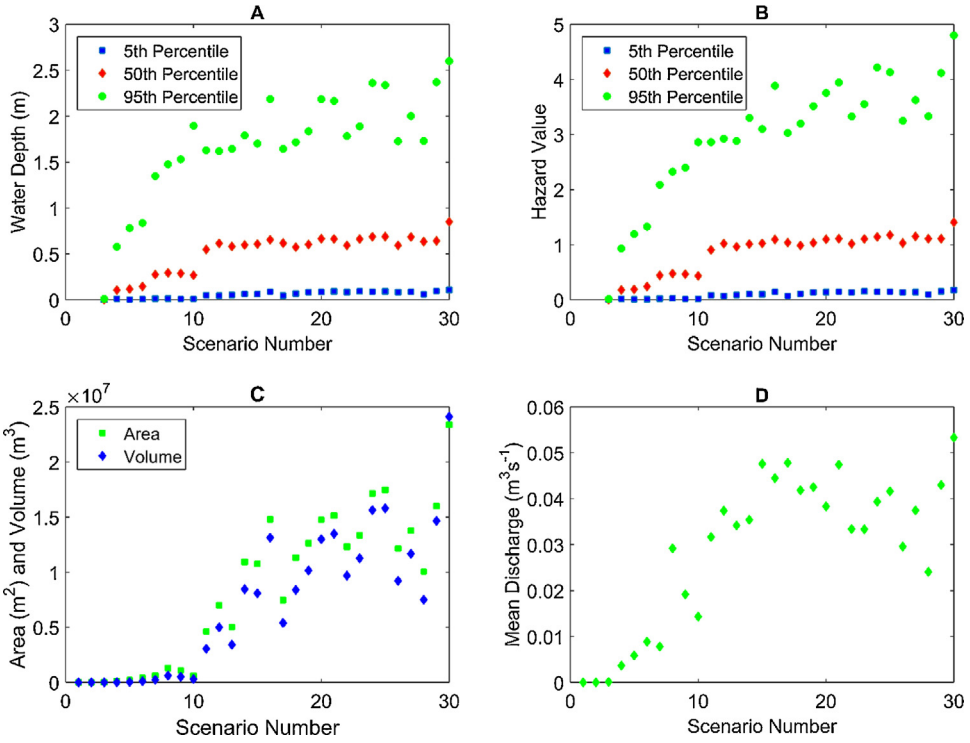

Fig. 3. (A) water depths, (B) hazard value, (C) area and volume and (D) mean discharge over defences for each of the 30 0.5% annual probability extreme events detailed in Table 1. Increasing scenario number equates to increasing WL and decreasing *Hs*. (For interpretation of the references to colour in text, the reader is referred to the web version of this article.)

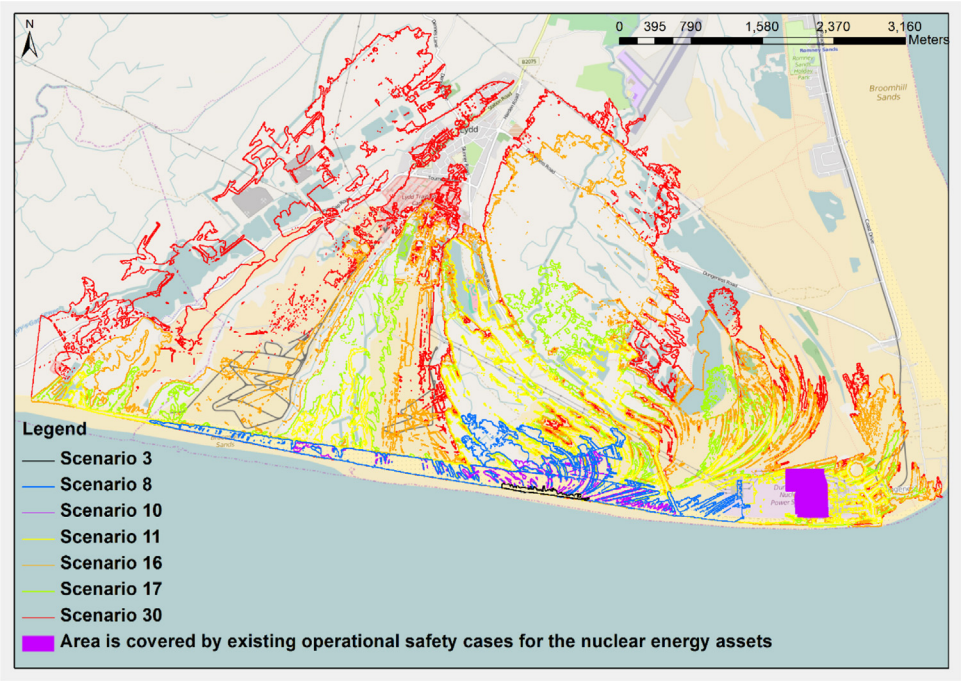

Fig. 4. Maximum flood extent outlines for Scenarios 3, 8, 10, 11, 16, 17 and 30. The purple area is covered by existing operational safety cases for the nuclear energy assets. (For interpretation of the references to colour in this figure legend, the reader is referred to the web version of this article.)

see the impact of this, but the computational cost in doing so meant it was not completed for this study.

Fig. 3 shows a distinctive trend of increasing area, volume, depths and hazard values for increasing scenario number. The first two scenarios show no overwashing of the defences, then in scenario 3 a slight increase in WL allows the largest waves (although slightly lower than in scenarios 1 and 2) to cause overwash. Fig. 3C shows a distinctive threshold or 'tipping point' between scenario 10 and 11 where the area and volume of the maximum inundation extent increase rapidly.

The values for inundation area and volume beyond scenario 10 show greater increase and scatter than the first 8 scenarios

(Fig. 3). Reductions in both area and volume occur for scenario 9 and 10 due to a reduction in *Tp* (Table 1) causing fewer profiles to overwash, and those that do to overwash with a reduced discharge.

Beyond scenario 10 (Fig. 3C) the greater variability in results is due to the variable *Tp*. Reduced inundation area and volume are associated with lower wave periods. Examples of this are between scenarios 16 and 17 (Fig. 4), which represent a 1.4 s decrease in *Tp*; this occurs between scenarios 21 and 22 and also 25 and 26 (Fig. 3C) where decreases in *Tp* of 0.5 s leads to an associated decrease in area and volume. The longer wave periods cause greater flood area and volume. This is most apparent between scenarios 10 and 11 but also for scenario 29 and 30, which are noticeably higher than the trend from scenario 10 onwards. It is suggested scenario 28 marks the transition from small wind waves to swell waves and another 'tipping point' for much larger flood extents. For the two sets of scenarios 10 to 11 and 29 to 30 the increases in *Tp* in 3.3 and 3.4 s, respectively, combined with the small increases in WL, 0.03 m and 0.08 m respectively, and large decreases in *Hs*, 0.37 m and 0.13 m respectively, shows that wave period has a large effect on defence overwashing discharge.

4.3. Variation in flood water depths and hazard value

Fig. 3A and 3B show similar trends since the hazard value is proportional to the water depth. The tipping point beyond scenario 10 (see Fig. 3C) is also apparent in these figures, although it is most evident in the 50th percentile data series. Again, more scatter is noticed beyond scenario 10 within all the data series. The decreasing trend (8–10) in the extent (Fig. 3C) is also weakly evident in the depths and hazard values (Fig. 3A and B) for the 50th and 5th percentile values. Beyond scenario 10, unlike Fig. 3C, the rate of increase in depth and hazard plateaus. This is likely a consequence of the much larger flood extents (after scenario 10) that breach the secondary defence (Green Wall) having a shallow depth. Since the hazard value trends correlate to depth, here we only discuss the change in trend to the depth, which in turn influences the hazard.

From scenarios 1 to 6 there is little change in flood extent, low water levels limit the ability of waves to overwash. Flooding first occurs in scenario 3 (Fig. 3A), at a point approximately 3 km east of the energy infrastructure towards the middle of the model domain. This demonstrates that the gravel barrier provides a lower level of protection than the augmented gravel barrier defending the critical infrastructure, which remain resilient. Overwash fans in later scenarios develop to the east and west of this point (e.g., scenario 8, Fig. 4).

The outline for scenario 11 (yellow) is much larger than scenario 10 (purple) (Fig. 4). Up to this point the inundation has been largely contained by the Green Wall secondary defence. These secondary defences restrict growth in the extent of flooding and enable the flood water depth to increase until these defences are also exceeded, most noticeably in scenario 11, causing a state change in the inundation extent and depth trends. The extent and volume can rapidly increase in the unconstrained state (Fig. 3A, 4), while the depth remains shallow in the spreading water (Fig. 3C). This explains the why the 95th percentile water depth, representative of the constrained water, for scenario 8–10 increases, peaking at scenario 10, despite the reduction in area and volume due to shorter wave periods limiting the number of overwash fans. Scenario 11 noticeably breaches these secondary defences which results in a much greater extent and volume but a reduction in the percentile flood water depths, which is most clearly reflected in the 95th percentile water depth value representing a large proportion of the outer area of the flooded region. Lower percentiles represent the shallow unconstrained depths towards the outer edge of inundation. The divergence in the percentile depth lines after scenario 10 suggests there is a large shallow outer margin to the spreading flood water, and that the coastal areas remain deep due to the constraining Green Wall.

Beyond scenario 11 the increase in flood depth is again quite constant, while the area and volume increases. This suggests the increase in overwashing causes the flood water to spread with a consistent depth over the domain. There is a noticeable dip in the inundation area and volume for scenario 17, again this is associated with waves of lowest period. For the larger extents, variability will also occur as new pathways become accessible to the flood water, enabling it to advance inland.

5. Discussion

5.1. Previous research

There has been a large amount of research into the behaviour of gravel barriers and beaches during extreme events. Physical modelling has been used to investigate morphological barrier response to wave and WL conditions (Matias et al., 2014). While numerical models have also been developed to simulate gravel barrier and beach response to storms. Recent research has found that XBeach-G provides a good prediction of wave run-up and initial overtopping (McCall et al., 2014) and can be applied to predict storm impacts on gravel beaches and barriers with reasonable confidence for a range of forcing conditions (McCall et al., 2015). However, this work has only focused only on the beach or barrier, and does not attempt to quantify the impact of storms on the areas at risk of inundation behind the defences. Research in coastal inundation still commonly only considers EWL, e.g. (Lewis et al., 2011; Wadey et al., 2015, 2013). While wave run-up and overwashing are present in some studies it tends to be in coupled modelling studies which require substantial resources to undertake (Stansby et al., 2013).

Using combined waves and WL, in addition with joint probability analysis, is not common in academic literature although examples do exist (Wadey et al., 2015). However, it is more widely used in commercial flood risk studies (EDF, 2012). Making the results and conclusions drawn from this study useful and applicable to decision makers when redesigning or upgrading coastal defences or shoreline management policy.

5.2. Effect of wave period on inundation

It is well known that wave period has a significant effect on wave run-up and overwash (Stockdon et al., 2006). However, since swell wave period for the continually decreasing wave height remains at a similar value (10 s) for the largest wind waves it is suggested that the main factor changing the flood inundation is the WL, and that 3.8 m total water level is the trigger level for waves of ~5 m to overwash the defences in this case (Scenario 3). The noticeable change in flood inundation between scenario 10 and 11 is thought to be in consequence of the increase in *Tp*, since scenario 8 has a similar mean overwash discharge to scenario 11.

Scenario 30, which has the maximum in all flood inundation parameters and longest swell wave period (of 16.7 s), was repeated with a smaller, typical wind wave period (of 2.8 s). The re-simulation caused no overwashing. Since swell waves coincident with high water levels cause the highest flood hazard and the rate of increase in the hazard seems related to the increase in extreme water level, it is suggested that trends in sea-level rise will translate directly into hazard rating. Changes in the swell component of the wave climate may also cause a greater hazard if long period waves become more frequent or severe. Other

changes in wave climate (e.g., direction) may also influence the uncertainty and probability of event occurrence.

5.3. Limitations of research

Limitations of this research are the short (12 year) wave record, reducing the confidence in the joint probability analysis to generate occurrence curves of 0.5% probability. The location of the data also limits the accuracy as it's restricted to points of observation. To address both limitations a long-term coupled wave-surge model would have been required. Since this research focuses on flood hazard for management purposes, the study has been limited to using coastal monitoring available to coastal managers within the UK. Correction for sea-level rise in the WL values has not been considered in this short dataset for the joint probability analysis. For this near-decadal record the change in mean sea level is of the order 2.6 cm (rising at approximately 2.18 mm/yr at Dover) (Woodworth and Williams, 2009). For analysis beyond a decade it is suggested sea-level rise should be considered to allow better comparison of historic events over the time (Wadey et al., 2014). Wave direction, which influences run-up and beach profile response, was not considered. Considering offshore wave direction prior to the joint probability analysis to remove *Hs* values from directions that have limited impact for this coastal geography would also improve the accuracy of the wave boundary forcing but limit the data available to identify low probability events with confidence. Deciding where to extract the discharge from the time-evolving beach profile is also difficult. In this study the defence crest in the profile at the end of the simulation was used to define the point where the discharge was extracted from the storm impact output to ensure consistency at a point that represented defence overwash throughout the simulation.

6. Conclusions

The results show that the greatest flood hazard to a location is due to low swell waves with the longest periods during extreme water levels, rather than large short period wind waves occurring at lower water levels. The analysis has shown that increasing water levels drives increasing overwash discharge for large wind waves. For this case study when the *Hs* is nearly equivalent to the WL (Scenario 15, *Hs* = 4.42 m, *Tp* = 10.0 s, WL = 4.34 m) a 'tipping point' is reached and the reduction in wind wave height reduces the overwash discharge. Then, once a swell wave regime is reached (Scenario 29, *Hs* = 1.05 m, *Tp* = 13.3 s, WL = 5.2 m), a second 'tipping point' is reached and the discharge increases in response to much longer wave periods. For the scenarios considered longer wave periods drive higher overwashing rates and thus flood inundation extents, and create the upper level in the scatter seen in the results. For this gravel barrier, with crest height between 5.70 m and 6.96 m, a 'tipping point' in flood extent is associated with the breach of the secondary defence which occurs for 10 s waves (Scenario 8 to 10) with WL = 3.2 m and *Hs* = 5.55 ranging to WL = 3.8 m and *Hs* = 5.02 m offshore.

Although all events simulated had the same annual probability of occurrence (0.5%) the flood hazard rating varied from 'none' to 'danger to all'. This study shows that relying on a single representation of a return period standard of protection is therefore too simplistic. Applying the methods presented to other locations would help with the decision making in refurbishing or building of new defences while also reducing the uncertainty in what the defences need to be resilient too. This will ensure the defences are not over- or under-engineered to cope with a 0.5% annual probability event, thus giving coastal managers and stakeholders more confidence of the sea defence resilience to this level of protection. Here we show water elevation is the main source of increased flood risk in locations dominated by wind waves. While swell waves pose the highest flood hazard, this is only when water levels are most extreme.

Acknowledgements

We would like to acknowledge the ESPRC-funded ARCC "Adaptation and Resilience of Coastal Energy Supply" (ARCoES) project (EPSRC EP/I035390/1) and the ERIIP "Sandscaping for Mitigating Coastal Flood and Erosion Risk to Energy Infrastructure on Gravel Shorelines: a case study approach" project (NERC NE/M008061/1) in partnership with the Crown Estate. We would also like to acknowledge Cefas' role in providing the wave data. Finally, we gratefully acknowledge the contributions of Tom Dauben, a local EA representative, for highlighting potential study locations.

References

Bates, P., De Roo, A.P., 2000. A simple raster-based model for flood inundation simulation. J. Hydrol. 236, 54–77. doi:http://dx.doi.org/10.1016/S0022-1694(00)00278-X.

Bates, P.D., Horritt, M.S., Fewtrell, T.J., 2010. A simple inertial formulation of the shallow water equations for efficient two-dimensional flood inundation modelling. J. Hydrol. 387, 33–45. doi:http://dx.doi.org/10.1016/j.jhydrol.2010.03.027.

BODC, 2015. Download UK Tide Gauge Network Data from BODC [WWW Document]. URL http://www.bodc.ac.uk/data/online_delivery/ntslf/ (accessed 18.01.16.).

Bradbury, A.P., Powell, K.A., 1992. The short term profile response of shingle spits to storm wave action. Coastal Eng. Proc. doi:http://dx.doi.org/10.9753/icce.v23.%p.

Buijs, F., Simm, J., Wallis, M., Sayers, P., 2007. Performance and reliability of flood and coastal defences.

Cefas—WaveNet [WWW Document]. URL https://www.cefas.co.uk/cefas-data-hub/wavenet/ (accessed 18.01.16.).

Chini, N., Stansby, P.K., 2012. Extreme values of coastal wave overtopping accounting for climate change and sea level rise. Coastal Eng. 65, 27–37. doi:http://dx.doi.org/10.1016/j.coastaleng.2012.02.009.

Coles, S.G., Tawn, J.A., 1990. Statistics of coastal flood prevention. Philos. Trans. R. Soc. A Math. Phys. Eng. Sci. 332, 457–476. doi:http://dx.doi.org/10.1098/rsta.1990.0126.

Dombusch, U., Williams, R., Moses, C., 2003. Beach material properties [www document]. Univ. Sussex URL http://www.sussex.ac.uk/geography/researchprojects/BAR/publish/Phase-1-final-beach material properties.pdf (accessed 18.01.16).

EDF, 2012. EU Stress Test Dungeness B [WWW Document]. URL https://www.edfenergy.com/sites/default/files/jer-srt-stt-pub-fin-001_dnb_stress_test_v1.1.pdf (accessed 18.01.16.).

Hames, D., Reeve, D., 2007. The joint probability of waves and high sea levels in coastal defence. Proc. Flood Risk Assess. II Conf. Inst. Math. Its Appl. Southend Sea 97–106.

Hawkes, P.J., Gouldby, B.P., 1998. The joint probability of waves and water levels: JOIN-SEA Version 1.0—User manual.

Hawkes, P.J., Svensson, C., 2006. Joint Probability: Dependence Mapping and Best Practice. HR Wallingford.

JNCC, 2015. Dungeness – Special Area of Conservation – SAC – Habitats Directive [WWW Document]. URL http://jncc.defra.gov.uk/protectedsites/sacselection/sac.asp?EUCode=UK0013059 (accessed 18.01.16.).

Lewis, M., Horsburgh, K., Bates, P., Smith, R., 2011. Quantifying the uncertainty in future coastal flood risk estimates for the U.K. J. Coastal Res. 276, 870–881. doi:http://dx.doi.org/10.2112/JCOASTRES-D-10-00147.1.

Long, A.J., Waller, M.P., Plater, A.J., 2007. Dungeness and the Romney Marsh: Barrier Dynamics and Marshland Evolution. Oxbow Books.

Longuet-Higgins, M.S., 1970. Longshore currents generated by obliquely incident sea waves: 1. J. Geophys. Res. 75, 6778–6789. doi:http://dx.doi.org/10.1029/JC075i033p06778.

Mason, T., Bradbury, A., Poate, T., Newman, R., 2009. Nearshore wave climate of the english channel—evidence for bi-modal seas. Coastal Engineering 2008. World Scientific Publishing Company, pp. 605–616. doi:http://dx.doi.org/10.1142/9789814277426_0051.

Matias, A., Blenkinsopp, C.E., Masselink, G., 2014. Detailed investigation of overwash on a gravel barrier. Mar. Geol. 350, 27–38. doi:http://dx.doi.org/10.1016/j.margeo.2014.01.009.

McCall, R.T., Masselink, G., Poate, T.G., Roelvink, J.A., Almeida, L.P., 2015. Modelling the morphodynamics of gravel beaches during storms with XBeach-G. Coastal Eng. 103, 52–66. doi:http://dx.doi.org/10.1016/j.coastaleng.2015.06.002.

McCall, R.T., Masselink, G., Poate, T.G., Roelvink, J.A., Almeida, L.P., Davidson, M., Russell, P.E., 2014. Modelling storm hydrodynamics on gravel beaches with

XBeach-G. Coast. Eng. 91, 231–250. doi:http://dx.doi.org/10.1016/j.coastaleng.2014.06.007.
McInnes, K.L., Walsh, K.J.E., Hubbert, G.D., Beer, T., 2003. Impact of sea-level rise and storm surges on a coastal community. Nat. Hazards 30, 187–207. doi:http://dx.doi.org/10.1023/A:1026118417752.
McMillan, A., Batstone, C., Worth, D., Tawn, J., 2011. Coastal flood boundary conditions for UK mainland and islands. Project SC060064/TR2: Design sea levels.
Natural England, 2015. Natural England Designated Sites View Dungeness, Romney Marsh and Rye Bay [WWW Document]. URL https://designatedsites.naturalengland.org.uk/SiteDetail.aspx?SiteCode=S2000533&SiteName=Dungeness&countyCode=&responsiblePerson= (accessed 18.01.16.).
NTSLF, 2015. National Tidal and Sea Level Facility [WWW Document]. URL https://www.ntslf.org/ (accessed 19.01.16.).
Palmer, T., Nicholls, R.J., Wells, N.C., Saulter, A., Mason, T., 2014. Identification of energetic swell waves in a tidal strait. Cont. Shelf Res. 88, 203–215. doi:http://dx.doi.org/10.1016/j.csr.2014.08.004.
Prime, T., Brown, J.M., Plater, A.J., 2015. Physical and economic impacts of sea-level rise and low probability flooding events on coastal communities. PLoS One 10, e0117030. doi:http://dx.doi.org/10.1371/journal.pone.0117030.
Quinn, N., Lewis, M., Wadey, M.P., Haigh, I.D., 2014. Assessing the temporal variability in extreme storm-tide time series for coastal flood risk assessment. J. Geophys. Res. Oceans 119, 4983–4998. doi:http://dx.doi.org/10.1002/2014JC010197.
D. Ramsbottom, D., 2003. Flood risks to people: phase1.
Skinner, C.J., Coulthard, T.J., Parsons, D.R., Ramirez, J.A., Mullen, L., Manson, S., 2015. Simulating tidal and storm surge hydraulics with a simple 2D inertia based model, in the Humber Estuary, U.K. Estuarine Coastal Shelf Sci. 155, 126–136. doi:http://dx.doi.org/10.1016/j.ecss.2015.01.019.
Stansby, P., Chini, N., Apsley, D., Borthwick, A., Bricheno, L., Horrillo-Caraballo, J., McCabe, M., Reeve, D., Rogers, B.D., Saulter, A., Scott, A., Wilson, C., Wolf, J., Yan, K., 2013. An integrated model system for coastal flood prediction with a case history for Walcot. UK, on 9 November 2007. J. Flood Risk Manag. 6, 229–252. doi:http://dx.doi.org/10.1111/jfr3.12001.
Stockdon, H.F., Holman, R.A., Howd, P.A., Sallenger, A.H., 2006. Empirical parameterization of setup, swash, and runup. Coastal Eng. 53, 573–588. doi:http://dx.doi.org/10.1016/j.coastaleng.2005.12.005.
Wadey, M.P., Brown, J.M., Haigh, I.D., Dolphin, T., Wisse, P., 2015. Assessment and comparison of extreme sea levels and waves during the 2013/14 storm season in two UK coastal regions. Nat. Hazards Earth Syst. Sci. 15, 2209–2225. doi:http://dx.doi.org/10.5194/nhess-15-2209-2015.
Wadey, M.P., Haigh, I.D., Brown, J.M., 2014. A century of sea level data and the UK's 2013/14 storm surges: an assessment of extremes and clustering using the Newlyn tide gauge record. Ocean Sci. 10, 1031–1045. doi:http://dx.doi.org/10.5194/os-10-1031-2014.
Wadey, M.P., Nicholls, R.J., Haigh, I., 2013. Understanding a coastal flood event: the 10th March 2008 storm surge event in the SolentUK. Nat. Hazards 10. . 1007/s11069-013-0610-5 http://dx.doi.org/10.1007/s11069-013-0610-5.
Wells, N.C., 2011. The Atmosphere and Ocean: A Physical Introduction. John Wiley & Sons.
Woodworth, P.L., Williams, S.D.P., 2009. Trends in UK Mean Sea Level Revisited. Geophys. J. Int. doi:http://dx.doi.org/10.1111/j.1365-246X.2008.03942 http://dx.doi.org/10.1111/j.1365-246X.2008.03942.
Wyse, I.A./G.A./P., 2015. Flood Map – your questions answered.